Carbohydrate Polymers 89 (2012) 307–313

Contents lists available at SciVerse ScienceDirect

Carbohydrate Polymers

journal homepage: www.elsevier.com/locate/carbpol

Quaternized chitosan-layered silicate intercalated composites based nanofibrous mats and their antibacterial activity

Hongbing Deng[a,b,1], Penghua Lin[b,1], Shangjing Xin[a], Rong Huang[a], Wei Li[a], Yumin Du[b], Xue Zhou[c,*], Jianhong Yang[d,b,**]

[a] College of Food Science and Technology, Huazhong Agricultural University, No. 1 Shizishan Road, Wuhan 430070, China
[b] School of Resource and Environmental Science, Wuhan University, Wuhan 430079, China
[c] Department of Occupational and Environmental Health and the MOE Key Laboratory of Environment and Health, School of Public Health, Tongji Medical College, Huazhong University of Science and Technology, Wuhan 430030, China
[d] School of Environmental and Safety Engineering, Changzhou University, Changzhou 213164, China

ARTICLE INFO

Article history:
Received 27 December 2011
Received in revised form 30 January 2012
Accepted 4 February 2012
Available online 11 February 2012

Keywords:
Quaternized chitosan
Organic rectorite
Intercalation
Electrospinning
Antibacterial activity

ABSTRACT

Quaternized chitosan (HTCC)–organic rectorite (OREC) intercalated composites based electrospun nanofibrous mats were fabricated from HTCC–OREC/polyvinyl alcohol (PVA) solutions for the first time. The morphology, intercalated structure, and antibacterial activity of the as-spun mats were investigated. The transmission electron microscopy images taken from HTCC–OREC composites showed that HTCC chains were inside the OREC interlayer. Scanning electron microscopy results verified that more typical fibrous structure would be generated by adding OREC. Fourier transform infrared spectra and energy-dispersive X-ray spectroscopy results indicated that OREC existed in the HTCC–OREC/PVA nanofibrous mats. The intercalation structure in nanofibrous mats was confirmed by X-ray diffraction results, which confirmed that HTCC and PVA chains could intercalate into the interlayer of OREC. The antibacterial activity of the electrospun mats was enhanced when the amount of the OREC increased. Therefore, the novel ternary nanofibrous mats could be used in the field of food packaging and biomedical applications.

1. Introduction

A few months ago, an evaluation report about layered silicate especially bentonite (dioctahedral montmorillonite) published by European Food Safety Authority (EFSA), had verified the safety of bentonite as food additives and confirmed bentonite was effective in reducing milk aflatoxin (European Food Safety Authority, 2011). EFSA also pointed out that layered silicates were ubiquitous in the environment occurring as a natural soil component, so it was not expected that their applications would adversely affect the environment (European Food Safety Authority, 2011). Although no typical tolerance investigations with any other layered silicates were found in the literature, rectorite (REC), another kind of layered silicate, was supposed to be an ideal material to be used in food packaging and biomedical applications in future.

Based on our recent research results (Deng, Li et al., 2011; Deng, Wang et al., 2011), it could be noted that REC especially organic rectorite (OREC) modified from REC, had larger interlayer distance, better separable layer thickness and layer aspect ratio than montmorillonite (MMT) (Wang, Du, Luo, Lin, & Kennedy, 2007; Wang, Du, Luo et al., 2009; Wang, Du, Sun, & Liu, 2009; Wang, Pei, Du, & Li, 2008). The tunable interlayer distance of OREC could obviously affect the efficiency of its application, such as adsorption ability (Feng et al., 2010), bacteria inhibition (Deng, Li et al., 2011; Deng, Wang et al., 2011), drug controlled release (Wang et al., 2007; Wang, Liu, Wang, & Sun, 2011) and gene delivery (Wang et al., 2008). It was very interesting that the activity of the antibacterial agent could be enhanced by adding OREC (Deng, Li et al., 2011; Deng, Wang et al., 2011), because OREC based composites had higher surface area which could cause efficient contact and interaction with bacteria.

As it mentioned before, polymer/layered silicate composite nanofibers not only could combine the properties of both inorganic and organic materials together in nanofibrous mats, but also had characteristics of nanofibers such as ultrafine diameter, high surface area-to-volume ratio, three dimensional (3D) structure, etc. (Deng, Li et al., 2011; Deng, Wang et al., 2011; Ding, Kimura, Sato, Fujita, & Shiratori, 2004; Ding, Li, Fujita, & Shiratori, 2006). Therefore, many researchers had fabricated polymer/layered silicate composite nanofibers and used them in aerospace, biodegradable materials, catalysis, etc. (Marras, Kladi, Tsivintzelis, Zuburtikudis,

* Corresponding author. Tel.: +86 27 83693280; fax: +86 27 83693280.
** Corresponding author. +86 519 86330086; fax: +86 519 86330083.
E-mail addresses: xue.zhou@hust.edu.cn (X. Zhou), yangshenyang3@163.com (J. Yang).
[1] Co-first author with the same contribution to this work.

0144-8617/$ – see front matter © 2012 Elsevier Ltd. All rights reserved.
doi:10.1016/j.carbpol.2012.02.009

& Panayiotou, 2008; Njuguna & Pielichowski, 2004; Su, 2009; Wypych & Satyanarayana, 2005), and electrospinning technique as an efficient and simple method had been selected to fabricate those nanofibrous mats (Deng, Li et al., 2011).

In order to fabricate electrospun polymer/layered silicate nanofibrous mats for food packaging and biomedical applications, biopolymers such as polysaccharides were more favorable than synthetic polymers. As we know, chitosan (CS) was a kind of polysaccharide with several properties such as hemostatic activity (Bonferoni, Sandri, Rossi, Ferrari, & Caramella, 2009), non-toxicity (Bhattarai, Edmondson, Veiseh, Matsen, & Zhang, 2005), biodegradability (Yang, Chen, & Wang, 2009), and antibacterial activity (Deng, Li et al., 2011; Deng, Wang et al., 2011). Quaternized chitosan (HTCC), a water soluble derivative of CS, was found with better bacteria inhibition properties than CS (Qin et al., 2004; Wang, Du, Luo et al., 2009). But unfortunately, CS and HTCC were both hard to be directly electrospun into nanofibers because their spinnability via electrospinning was poor (Alipour, Nouri, Mokhtari, & Bahrami, 2009; Deng, Li et al., 2011; Geng, Kwon, & Jang, 2005). Therefore, polyvinyl alcohol (PVA) was added into the HTCC solutions to moderate the repelling interaction between HTCC and to enhance the molecular entanglement, as it was demonstrated to be effective in promoting fiber spinnability (Sajeev, Anand, Menon, & Nair, 2008; Zhang et al., 2007; Zhou, Yang, & Nie, 2007). Alipour et al. (2009) reported that the defect free nanofibrous mats were electrospun from an aqueous solution of PVA–HTCC blends. The average diameter of as-spun fibers was 200–600 nm, and it was decreased when HTCC content was increased in the blends. They also investigated the antibacterial activity of the prepared mats and verified that HTCC was an idea antibacterial material.

The present study described that a series of HTCC–OREC/PVA ternary intercalated composites based nanofibrous membranes were fabricated via electrospinning technique. The morphology of the as-spun mats and the effect of OREC on the antibacterial activity enhancement were examined.

2. Experimental

2.1. Materials

Chitosan (CS, $M_w = 2.0 \times 10^5$ kDa) from shrimp shell with 92% deacetylation was from Zhejiang Yuhuan Ocean Biochemical Co., China. Polyvinyl alcohol (PVA, $M_w = 9 \times 10^4$) was purchased from Sigma Aldrich Co., USA. Calcium rectorite (Ca^{2+}-REC) was provided by Hubei Mingliu Inc., Co. (Wuhan, China). All other chemicals were of analytical grade and were used as received without any further purification. All aqueous solutions were prepared using purified water with a resistance of 18.2 MΩ cm.

2.2. Synthesis of quarternized chitosan

The synthesis of quarternized chitosan was prepared by a previous method (Lim & Hudson, 2004). Briefly, CS (5 g) was dissolved into 2% (w/v) acetic acid (250 mL) and then adjusted the pH to 9.0 by NaOH to make chitosan separate out. After soaked 8 h, the solution was filtered to obtain purified CS. Then CS powder was transferred into a boiling flask and added by isopropyl (15 mL) and 2,3-epoxypropyl trimethylammonium chloride under gentle agitation in 80 °C bath as well. The product was washed by ethanol and the obtained solid was dialyzed against deionized water for 3 days and lyophilized to give N-(2-hydroxyl)propyl-3-trimethyl ammonium chitosan chloride (HTCC). The degree of substitution of the quaternization group was determined by capacity titration.

2.3. Preparation of intercalated composites

The organic rectorite (OREC) and intercalated HTCC–OREC were prepared according to our previous reports (Deng, Li et al., 2011; Deng, Wang et al., 2011). Briefly, OREC was prepared by sodium dodecylsulfonate cation exchange reactions. The OREC suspension was pretreated by ultrasonication. Then 7% HTCC solution prepared by dissolving HTCC in purified water was added dropwise and slowly into OREC suspension at 60 °C under gentle agitation for 12 h to obtain mixed solution. At last, the solution was filtered, and the precipitate was washed and dried under vacuum to get the composites.

2.4. Preparation of the spinning solutions

7% PVA solution was prepared by adding PVA in purified water at 60 °C bath with gentle magnetic stirring for 4 h. HTCC or HTCC–OREC was dissolved into purified water with constant agitation in close vials for 2 h at room temperature to obtain 2% solutions. The HTCC/PVA solutions were mixed with 7% HTCC and 7% PVA to obtain HTCC/PVA mixture at 80/20, 60/40, 50/50 and 40/60 mass ratios. All solutions were stirred for 24 h. The HTCC–OREC/PVA solutions were mixed at the same mass ratios of HTCC/PVA as above but containing 0.5%, 1% and 2% OREC, respectively. Then the mixtures were stirred for 48 h. The concentrations of all above solutions were expressed in wt./wt.%.

2.5. Fabrication of nanofibrous mats

The electrospinning process was similar as our previous report (Deng, Li et al., 2011). The applied voltage was 10 kV, the tip-to-collector distance was 15 cm, and the speed of deliver solutions was 1 mL/h. The as-spun fibers were collected by grounded cylindrical collector covered by aluminum foil. The ambient temperature and relative humidity were kept at 25 °C and 45%, respectively. The prepared samples were dried in vacuum at room temperature to remove the trace solvent for 24 h.

2.6. Characterization

The transmission electron microscopy images (TEM) of intercalated composites were obtained by JEM 2100 (JEOL, Japan). Fourier transform infrared (FT-IR) spectra were examined by a Nicolet FT-IR 5700 spectrophotometer (Nicolet, Madison, USA). The morphology of electrospun samples was observed by field-emission scanning electron microscope (FE-SEM, S-4800, Hitachi Ltd., Japan). The small angle X-ray diffraction (SAXRD) was performed on type D/max-rA diffractometer (Rigaku Co., Japan) with Cu target and Kα radiation (λ = 0.154 nm). The scanning rate was 1°/min and the scanning scope of 2θ was 1–10°.

2.7. Bacterial inhibition assay

Disk-diffusion method was used to investigate the inhibitory effect of the ternary films against Gram-negative bacteria *Escherichia coli* and Gram-positive bacteria *Staphylococcus aureus*. 50 μL bacteria levitation liquid with the concentration of $5.0–10.0 \times 10^5$ cfu/mL were added into meat-peptone broth and then coating uniformly. As-spun nanofibrous mats disks together with aluminum foil (diameter = 7 mm) were sterilized at 120 °C for 30 min, and then were tiled on meat-peptone broth to cling to the bacteria levitation liquid. After incubated at 37 °C for 24 h, the inhibition zones were measured with a tolerance of 1 mm. Each sample was repeated three times.

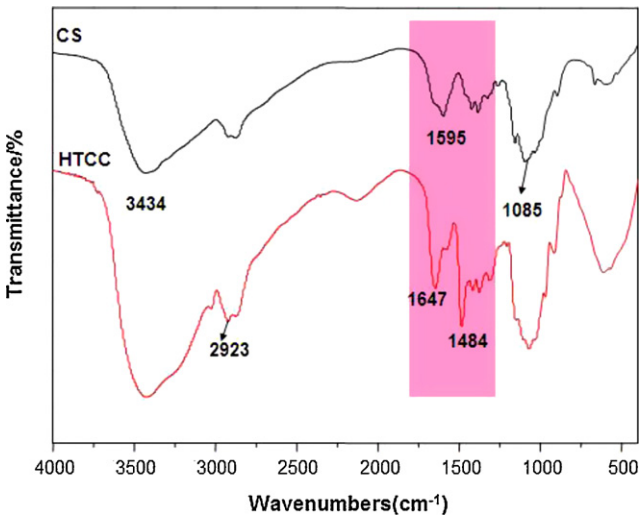

Fig. 1. FT-IR spectra of (a) CS and (b) HTCC modified from CS.

3. Results and discussion

In order to verify the synthesis of HTCC, FT-IR spectra of CS and samples modified from CS were shown in Fig. 1. CS had resonance peaks at 3423 confirmed the N—H stretching of the primary amino groups (Deng, Li et al., 2011; Lim & Hudson, 2004). Bands at 1657 and 1609 cm^{-1} commonly known as the C=O stretching of the secondary amide and $-NH_2$ bending of the primary amine, respectively. The band around 1085 cm^{-1} was assigned to the unsymmetric stretching of C—O—C. Fig. 1 also confirmed that the introduction of the quaternary ammonium salt group onto CS backbone was successful. Obviously, a new band occurred at 1484 cm^{-1}, which was attributed to the C—H bending of trimethylammonium group. The results were identical with the previous reports (Huang, Chen, Sun, Hu, & Gao, 2006; Lim & Hudson, 2004; Wang, Du, Luo et al., 2009).

In this study, the building of predesigned intercalated architecture of HTCC–OREC was important to the internal structure of the composited nanofibrous mats, and direct evidence of this nanometer-scale dispersion of intercalated OREC could be found in the TEM images taken from the HTCC–OREC composites, as exhibited in Fig. 2 with different magnifications. It can be observed that the platy structure of OREC was clearly and many OREC layers crossed over together. In Fig. 2b and c, the parallel dark lines indicated that OREC was agglomerated (Wang, Du, Luo et al., 2009). In Fig. 2c, the interlayer of the OREC has been intercalated by HTCC chains. It clearly demonstrated that the expected HTCC–OREC composites were fabricated.

Fig. 3 shows the FE-SEM images of fibrous membranes electrospun from HTCC/PVA mixture solutions at different mass ratios. The morphology, fiber diameter and amount of fibers were affected by the variation of the mixture compositions. The average diameter of fibers fabricated from HTCC/PVA (20/80) (Fig. 3a) were much thicker than that of the fibers fabricated from the solutions containing more HTCC (Fig. 3b–d), because HTCC could not be directly electrospun in water solvent. In addition, bead-like structure could be observed in the nanofibrous mats and the average diameter of spun-nanofibers decreased when HTCC content increased in the mixed solution. The results suggested that although fibers could not be electrospun from the HTCC alone in purified water, adding PVA to the solutions enabled fiber formation.

Fig. 4a–c represents the FE-SEM images of as-spun nanofibrous mats with the addition of OREC. In order to investigate the effect

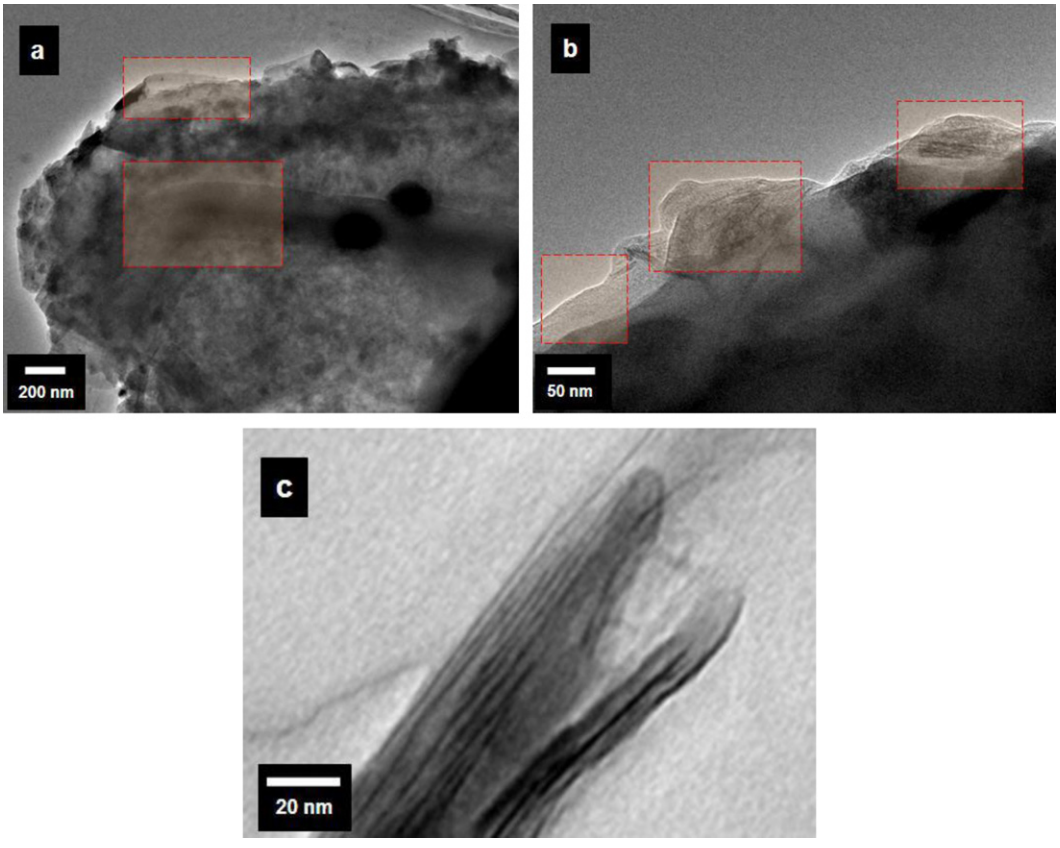

Fig. 2. TEM images taken from HTCC–OREC composites.

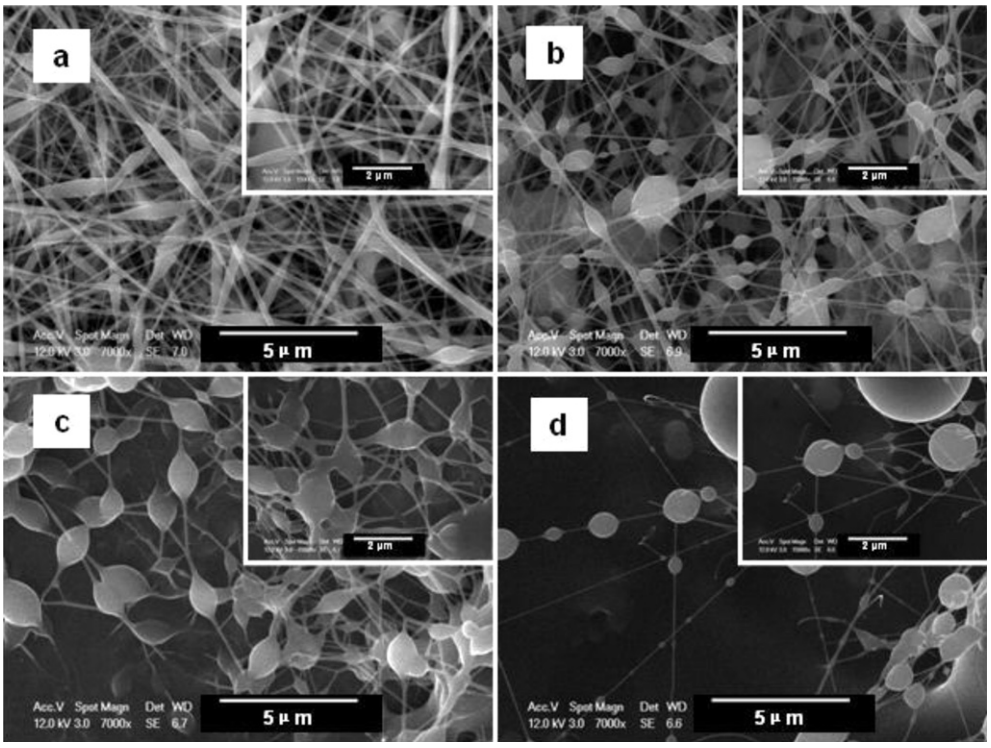

Fig. 3. FE-SEM images of nanofibrous mats electrospun from solutions with various HTCC/PVA mass ratios: (a) 20/80, (b) 40/60, (c) 50/50 and (d) 60/40.

of OREC amount on the fiber formation, various concentrations of OREC in the mixture were regulated at 0.5%, 1% and 2%. All the as-spun nanofibrous mats maintained typical fiber shape. When the concentration of OREC was at 2%, the undesirable OREC blocks were observed among the fibers. In addition, the morphology of as-spun fibrous mats had no visible difference between Fig. 4a and b. In Fig. 4d, EDX spectrum indicated that Si and Al elements were detected, which confirmed that OREC existed in the nanofibrous mats (Deng, Li et al., 2011; Deng, Wang et al., 2011).

Fig. 5 displays FE-SEM images of as-spun OREC contained fibrous mats. All HTCC–OREC/PVA solutions were fabricated fine, cylindrical, continuous, and randomly oriented fibers. The amount of

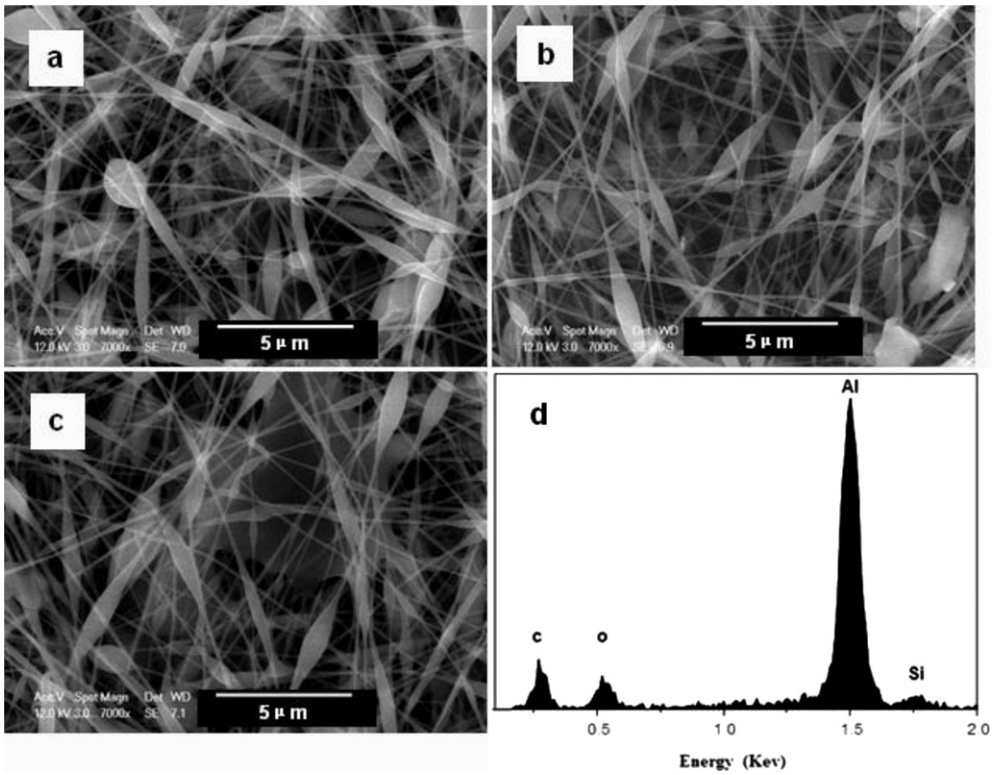

Fig. 4. FE-SEM images of nanofibrous mats fabricated from HTCC/PVA (40/60) mixture containing various content of OREC: (a) 0.5%, (b) 1%, (c) 2% and (d) EDX spectrum of selected area from sample b.

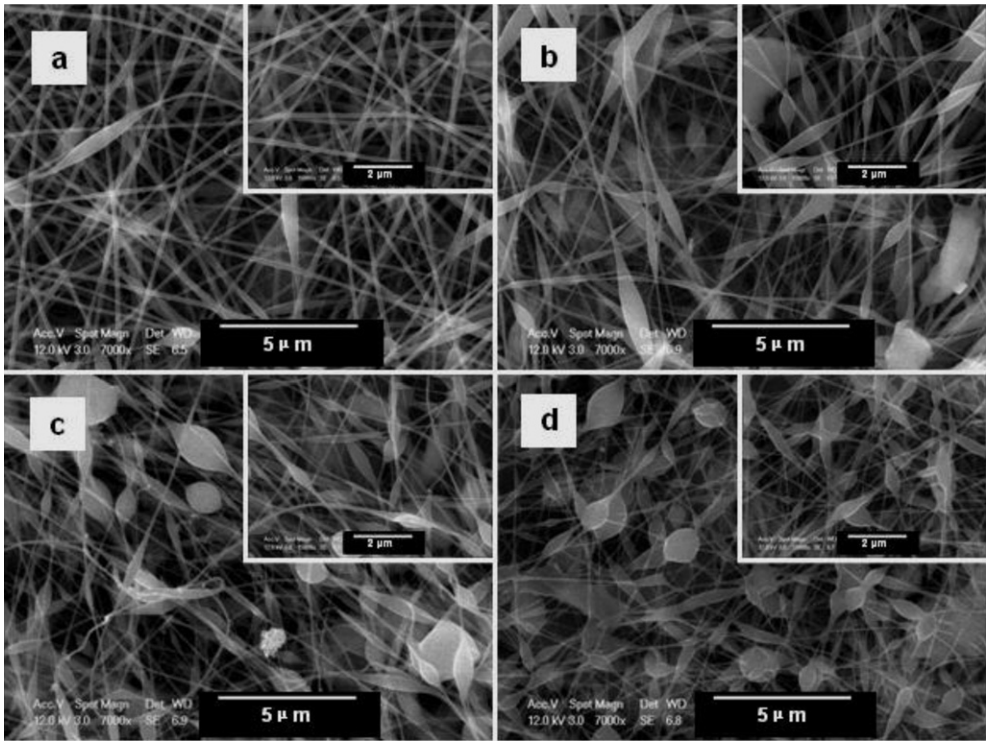

Fig. 5. FE-SEM images of nanofibrous mats electrospun from solutions with various HTCC/PVA mass ratios containing 1% OREC: (a) 20/80, (b) 40/60, (c) 50/50 and (d) 60/40.

fibers fabricated from HTCC–OREC/PVA solutions was more than that from HTCC/PVA solutions (Fig. 3). In Fig. 3d, there were few collectable fibers, but in Fig. 5d uniform fibrous mats containing several beads could be observed. An explanation for this was currently not clear. It was possible that OREC had interaction with HTCC and PVA chains, and the viscosity and conductivity of the solution had been changed. In addition, it was important to note that the beads would be less when OREC was added. A reason why this occurred was that the electrostatic repulsion forces would be enhanced by the increasing components in the mixture and overcame the surface tension at the tip of the needle in some locations where OREC existed. As previously noted fiber amount, OREC might be as a delicate balance which should be kept to ensure the fabrication of ideal fibers.

FT-IR spectra were taken from the bulk HTCC, PVA and OREC samples and the electrospun mats. As was shown in Fig. 6, PVA had the absorption bands at 3383, 2941, 1734, 1098, and 850 cm^{-1}, commonly known as the O—H, —CH_2, C═O, C—O, and C—C, respectively (Deng, Li et al., 2011; Li & Hsieh, 2006). OREC showed dominant peaks at 467 and 546 cm^{-1}, which were characteristic of Si—O bending vibration (Deng, Li et al., 2011). In the spectrum of HTCC–OREC/PVA nanofibrous mats (Fig. 6e), the band of OREC at 3643 cm^{-1} disappeared, which implied that the —OH of OREC may form ether bond with the —OH of HTCC or PVA, and possibly generated hydrogen bond with the amino group of HTCC. Moreover, the N—H bonded to O—H vibration band at 3448 cm^{-1} in HTCC shifted toward lower frequency no matter what it was mixed with, because the —NH_2 and —OH groups of HTCC formed hydrogen bonds with

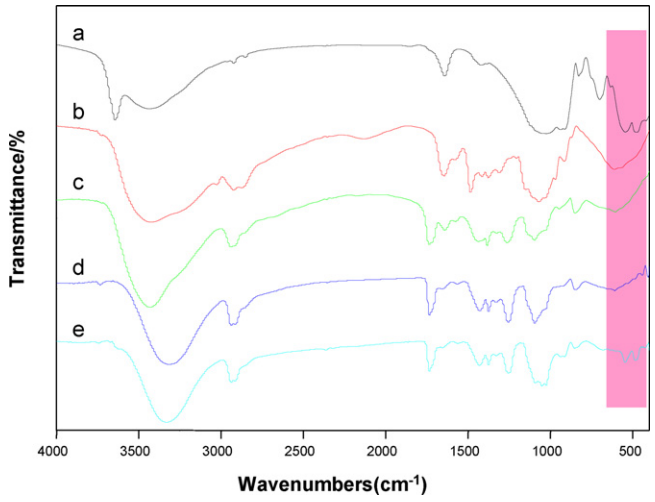

Fig. 6. FT-IR spectra of: (a) OREC powder, (b) HTCC powder, (c) PVA nanofibrous mats, (d) HTCC/PVA nanofibrous mats and (e) HTCC–OREC/PVA nanofibrous mats.

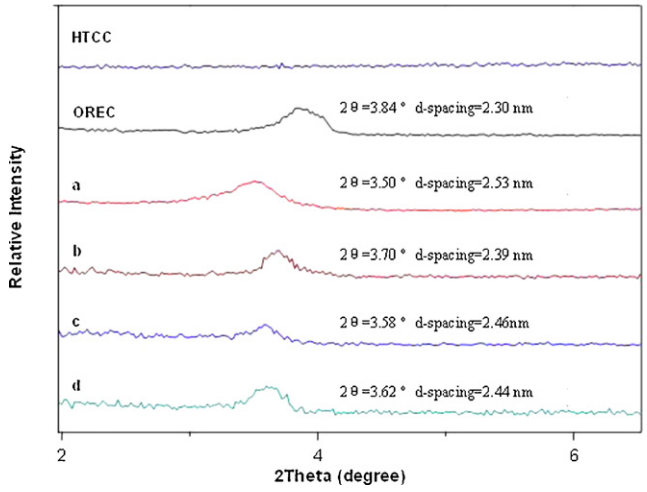

Fig. 7. SAXRD patterns of OREC powder, HTCC powder, PVA nanofibrous mats and (a) HTCC–OREC composites, and nanofibrous mats containing 1% OREC: (b) OREC/PVA, (c) HTCC–OREC/PVA = 80/20 and (d) HTCC–OREC/PVA = 60/40.

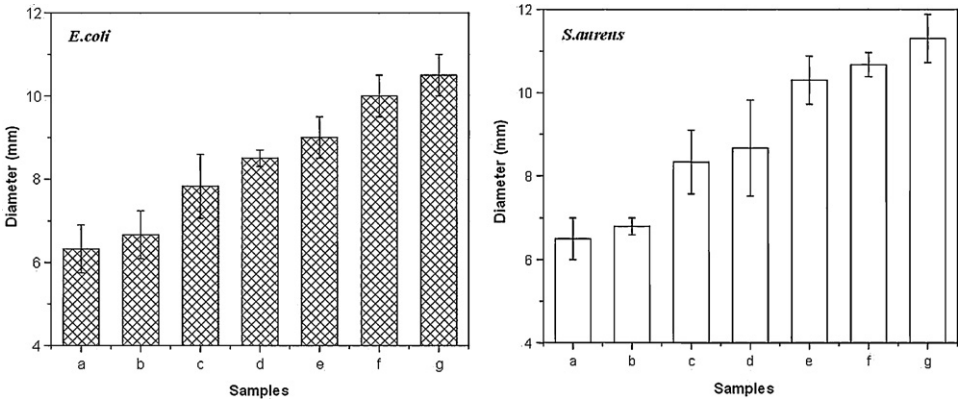

Fig. 8. Antimicrobial activities against *E. coli* and *S. aureus* of: (a) aluminum foil and mats electrospun from (b) PVA, (c) HTCC/PVA = 40/60, (d) HTCC/PVA = 60/40, (e) HTCC–OREC/PVA = 60/40 containing 0.5% OREC, (f) HTCC–OREC/PVA = 60/40 containing 1% OREC and (g) HTCC–OREC/PVA = 60/40 containing 2% OREC.

the —OH group of OREC and PVA. Hydrogen bonding interaction might generate between and inside HTCC molecules when they were constrained in the gallery of OREC layers, as seen in the spectra of the Fig. 6e with the largest loading of HTCC chains into the interlayer of OREC, where the N—H and O—H vibrations shifted to the lowest frequency (3419 cm^{-1}) (Deng, Li et al., 2011).

To further verify the expected intercalated architecture in composite nanofibrous mats, the SAXRD patterns of fibrous samples were recorded to measure the change of gallery distance of OREC before and after intercalation (Fig. 6). The distance between OREC was 2.30 nm, calculated by Bragg's equation. The SAXRD curves of the OREC based nanofibers diminished in comparison with the curve of OREC. HTCC resulted in a much bigger interlayer distance enlargement of OREC than PVA, because the cationic amido of HTCC intercalated into the interlayer of OREC generated electrostatic repulsion forces and compelled the distance of the interlayer to become large enough to accomplish a harmonious balance. For PVA chains there were merely general infiltration and hydrogen bonds (Deng, Li et al., 2011; Deng, Wang et al., 2011). As a result, HTCC was more efficient than PVA in the intercalation process.

The inhibition ability of the composite nanofibrous mats against *E. coli* and *S. aureus* was measured via inhibition zone surrounding circular mats disks and the results were shown in Fig. 7. Obviously, all HTCC contained nanofibrous mats had exhibited antibacterial activity. In addition, the as-spun mats showed better inhibitory property against the Gram-positive bacteria growth than that for Gram-negative bacteria when contained HTCC or OREC, and the results agreed with the previous studies (Alipour et al., 2009; Lim & Hudson, 2004; Wang, Du, Luo et al., 2009). Furthermore, aluminum foil disks were selected as the negative controls, and their diameters of inhibition zone were around 6.3 cm against *E. coli* and 6.5 cm against *S. aureus*, respectively, because aluminum foil disks were covered on the surface of the bacteria colonies and inhibited O_2 and CO_2 contacted with bacteria, so the bacteria would be killed. Based on the results of the inhibition zone diameters, it was obvious that the HTCC–OREC/PVA ternary nanofibrous mats exhibited better degree of growth inhibition than that of binary HTCC/PVA mats, and the PVA nanofibrous mats showed a little antibacterial activity. The results indicated that the ability of growth inhibition of the as-spun mats would be improved with the addition of OREC and also suggested that HTCC had much better antimicrobial activity than PVA. The enhancement of the bacterial inhibition by adding OREC was identical with previous reports (Wang et al., 2006; Deng, Li et al., 2011; Deng, Wang et al., 2011). Moreover, the degree of bacterial inhibition of as-prepared mats was enhanced when the content of OREC was increased (Fig. 8d–g), because OREC could absorb and inhibit the proliferation of bacteria on account of its significant surface area and adsorption capacities, and improved the antibacterial activity of nanofibrous mats (Wang, Du, Luo et al., 2009). Adsorption between silicate and bacteria was regarded as the main reason. Wang et al. also reported that when the amount of OREC increased, the effective layers per unit weight might increase owing to good dispersion. Therefore, larger specific surface area would exist and more bacteria were immobilized on the OREC surface (Wang, Du, Luo et al., 2009).

4. Conclusions

HTCC–OREC intercalated structure was established by solution intercalation method and then the composites were fabricated into nanofibrous mats via electrospinning technique successfully. The novel ternary composite as-spun nanofibrous mats were with good fiber shape and morphology, which were affected by the mass ratios of the three components in the electrospinning solutions obviously, especially by the addition of OREC. Moreover, OREC contained nanofibrous mats resulted in better bacterial inhibition activity than HTCC–PVA electrospun mats. Therefore, the HTCC–OREC/PVA ternary nanofibrous mats had great potential values in food packaging and biomedical applications.

Acknowledgment

This project was funded by National Natural Science Foundation of China (No. 31101365).

References

Alipour, S. M., Nouri, M., Mokhtari, J., & Bahrami, S. H. (2009). Electrospinning of poly(vinyl alcohol)–water-soluble quaternized chitosan derivative blend. *Carbohydrate Research*, *344*, 2496–2501.

Bhattarai, N., Edmondson, D., Veiseh, O., Matsen, F. A., & Zhang, M. Q. (2005). Electrospun chitosan-based nanofibers and their cellular compatibility. *Biomaterials*, *26*, 6176–6184.

Bonferoni, M. C., Sandri, G., Rossi, S., Ferrari, F., & Caramella, C. (2009). Chitosan and its salts for mucosal and transmucosal delivery. *Expert Opinion on Drug Delivery*, *6*, 923–939.

Deng, H. B., Li, X. Y., Ding, B., Du, Y. M., Li, G. X., Yang, J. H., et al. (2011). Fabrication of polymer/layered silicate intercalated nanofibrous mats and their bacterial inhibition activity. *Carbohydrate Polymers*, *83*, 973–978.

Deng, H. B., Wang, X. Y., Liu, P., Ding, B., Du, Y. M., Li, G. X., et al. (2011). Enhanced bacterial inhibition activity of layer-by-layer structured polysaccharide film-coated cellulose nanofibrous mats via addition of layered silicate. *Carbohydrate Polymers*, *83*, 239–245.

Ding, B., Kimura, E., Sato, T., Fujita, S., & Shiratori, S. (2004). Fabrication of blend biodegradable nanofibrous nonwoven mats via multi-jet electrospinning. *Polymer*, *45*, 1895–1902.

Ding, B., Li, C. R., Fujita, S., & Shiratori, S. (2006). Layer-by-layer self-assembled tubular films containing polyoxometalate on electrospun nanotibers. *Colloids and Surfaces A: Physicochemical and Engineering Aspects*, *284*, 257–262.

European Food Safety Authority (EFSA). (2011). Scientific opinion on the safety and efficacy of bentonite (dioctahedral montmorillonite) as feed additive for all species. *EFSA Journal*, *9*, 2007–2030.

Feng, Y. A., Gong, J. L., Zeng, G. M., Niu, Q. Y., Zhang, H. Y., Niu, C. G., et al. (2010). Adsorption of Cd (II) and Zn (II) from aqueous solutions using magnetic hydroxyapatite nanoparticles as adsorbents. *Chemical Engineering Journal*, *162*, 487–494.

Geng, X. Y., Kwon, O. H., & Jang, J. H. (2005). Electrospinning of chitosan dissolved in concentrated acetic acid solution. *Biomaterials*, *26*, 5427–5432.

Huang, R. H., Chen, G. H., Sun, M. K., Hu, Y. M., & Gao, C. J. (2006). Studies on nanofiltration membrane formed by diisocyanate cross-linking of quaternized chitosan on poly(acrylonitrile) (PAN) support. *Journal of Membrane Science*, *286*, 237–244.

Li, L., & Hsieh, Y. L. (2006). Chitosan bicomponent nanofibers and nanoporous fibers. *Carbohydrate Research*, *341*, 374–381.

Lim, S. H., & Hudson, S. M. (2004). Synthesis and antimicrobial activity of a water-soluble chitosan derivative with a fiber-reactive group. *Carbohydrate Research*, *339*, 313–319.

Marras, S. I., Kladi, K. P., Tsivintzelis, L., Zuburtikudis, I., & Panayiotou, C. (2008). Biodegradable polymer nanocomposites: The role of nanoclays on the thermomechanical characteristics and the electrospun fibrous structure. *Acta Biomaterialia*, *4*, 756–765.

Njuguna, J., & Pielichowski, K. (2004). Polymer nanocomposites for aerospace applications: Fabrication. *Advanced Engineering Materials*, *6*, 193–203.

Qin, C. Q., Xiao, Q., Li, H. R., Fang, M., Liu, Y., Chen, X. Y., et al. (2004). Calorimetric studies of the action of chitosan-N-2-hydroxypropyl trimethyl ammonium chloride on the growth of microorganisms. *International Journal of Biological Macromolecules*, *34*, 121–126.

Sajeev, U. S., Anand, K. A., Menon, D., & Nair, S. (2008). Control of nanostructures in PVA PVA/chitosan blends and PCL through electrospinning. *Bulletin of Materials Science*, *31*, 343–351.

Su, D. S. (2009). The use of natural materials in nanocarbon synthesis. *ChemSusChem*, *2*, 1009–1020.

Wang, X. Y., Du, Y. M., Luo, J. W., Lin, B. F., & Kennedy, J. F. (2007). Chitosan/organic rectorite nanocomposite films: Structure, characteristic and drug delivery behaviour. *Carbohydrate Polymers*, *69*, 41–49.

Wang, X. Y., Du, Y. M., Luo, J. W., Yang, J. H., Wang, W. P., & Kennedy, J. F. (2009). A novel biopolymer/rectorite nanocomposite with antimicrobial activity. *Carbohydrate Polymers*, *77*, 449–456.

Wang, X. Y., Du, Y. M., Sun, R. C., & Liu, C. F. (2009). Antimicrobial activity of quaternized chitosan/organic rectorite nanocomposite. *Journal of Inorganic Materials*, *24*, 1236–1242.

Wang, X. Y., Du, Y. M., Yang, H. H., Wang, X. H., Shi, X. W., & Hu, Y. (2006). Preparation, characterization and antimicrobial activity of chitosan/layered silicate nanocomposites. *Polymer*, *47*, 6738–6744.

Wang, X. Y., Liu, B., Wang, X. H., & Sun, R. C. (2011). Amphoteric polymer–clay nanocomposites with drug-controlled release property. *Current Nanoscience*, *7*, 183–190.

Wang, X. Y., Pei, X. F., Du, Y. M., & Li, Y. (2008). Quaternized chitosan/rectorite intercalative materials for a gene delivery system. *Nanotechnology*, *19*.

Wypych, F., & Satyanarayana, K. G. (2005). Functionalization of single layers and nanofibers: A new strategy to produce polymer nanocomposites with optimized properties. *Journal of Colloid and Interface Science*, *285*, 532–543.

Yang, X. C., Chen, X. N., & Wang, H. J. (2009). Acceleration of osteogenic differentiation of preosteoblastic cells by chitosan containing nanofibrous scaffolds. *Biomacromolecules*, *10*, 2772–2778.

Zhang, Y. Y., Huang, X. B., Duan, B., Wu, L. L., Li, S., & Yuan, X. Y. (2007). Preparation of electrospun chitosan/poly(vinyl alcohol) membranes. *Colloid and Polymer Science*, *285*, 855–863.

Zhou, Y. S, Yang, D. Z., & Nie, J. (2007). Effect of PVA content on morphology, swelling and mechanical property of crosslinked chitosan/PVA nanofibre. *Plastics Rubber and Composites*, *36*, 254–258.